Tandem Heterocyclization Activity of the Multidomain 230 kDa HMWP2 Subunit of *Yersinia pestis* Yersiniabactin Synthetase: Interaction of the 1−1382 and 1383−2035 Fragments†

Zucai Suo,‡ Christopher T. Walsh,* and Deborah Ann Miller‡

Department of Biological Chemistry and Molecular Pharmacology, Harvard Medical School, Boston, Massachusetts 02115

Received July 8, 1999

ABSTRACT: The six-domain, 2035-amino acid subunit high-molecular weight protein 2 (HMWP2) activates salicylate and two cysteines and loads them covalently on its three carrier protein domains during assembly of the iron-chelating virulence factor, yersiniabactin of the plague bacterium *Yersinia pestis*. The 1−1382 fragment of HMWP2 (ArCP−Cy1-A), overproduced in *Escherichia coli*, contains the first three domains: the aryl carrier protein (ArCP) domain, the cysteine specific adenylation domain (A), and the first condensation/cyclization domain (Cy1). The ArCP can be posttranslationally phosphopantetheinylated on Ser52 and then loaded with a salicyl group on the phosphopantetheine (Ppant) thiol by action of the YbtE, a salicyl-AMP ligase. The HMWP2 1−1382 fragment can activate L-cysteine as Cys-AMP. The HMWP2 1383−2035 fragment contains the remaining three domains: two peptidyl carrier proteins (PCP1 and PCP2) separated by a second condensation/cyclization domain (Cy2). Phosphopantetheinylation of the HMWP2 1383−2035 fragment at Ser1439 (PCP1) and Ser1977 (PCP2) facilitates cysteinylation of both thiols by HMWP2 1−1382. When the holo 1−1382 and bis-holo 1383−2035 protein fragments are mixed with ATP, salicylate, and cysteine, four products are slowly released [salicylcysteine (Sal-Cys), **(**hydroxyphenylthiazolinyl)cysteine (HPT-Cys), HPT-Cys-Cys, and the bisheterocyclic HPTT-Cys], reflecting thiolytic rerouting by cysteine in solution of elongating acyl-S-enzyme intermediates tethered at ArCP, PCP1, and PCP2 carrier protein domains, respectively. Conducting the in trans reconstitution with the S1439A mutant of HMWP2 1383−2035 releases only Sal-Cys, while the S1977A mutant leads to HPT-Cys formation but not HPT-Cys-Cys or HPTT-Cys. These results suggest localization of particular acyl-S-enzyme intermediates to each of the three carrier protein regions and also establish the sequential action of Cy1 and Cy2, with the latter producing the tandem 4,2-bisheterocyclic hydroxyphenylthiazolinylthiazolinyl (HPTT) moiety characteristic of this class of siderophores.

Yersiniabactin (Ybt), **1** (*1*, *2*), is the iron-chelating siderophore produced under iron starvation conditions by the Gram-negative *Yersinia* bacteria, including the pathogen of human plague, *Yersinia pestis* (*3*−*5*). Ybt biosynthetic genes are clustered in a high-pathogenicity island (*5*, *6*), and interruption of Ybt production markedly attenuates *Yersinia* virulence in animal infections (*5*−*8*). The presumed coordination sites for iron [$K_D = 10^{-35}$ M (R. D. Perry and L. E. DeMoll, unpublished result)] include the phenol, the thiazolidine nitrogen, the two thiazoline nitrogens, and the free carboxylate (Scheme 1). These four rings have been predicted to arise from the biosynthetic precursors salicylate and three cysteines. This expectation has been supported by inspection of the domain organization of the two multimodular proteins, high-molecular weight proteins 1 and 2 (HMWP1[1] and HMWP2, respectively) that encode Ybt assembly (*9*−*11*). In particular, HMWP2 (Figure 1) is a six-domain, 2035-amino acid (aa), 230 kDa protein with typical nonribosomal protein synthetase (NRPS) organization [peptidyl carrier protein (PCP), adenylation (A), and condensation/cyclization (Cy) domains (*9*, *11*)], while HMWP1 is a 3163-amino acid, 350 kDa protein with nine proposed domains, the first five being similar to polyketide synthases (PKS) that activate malonyl groups before terminating with four NRPS domains. As in other assembly lines of multidomain synthetases (*12*−*15*), domain order provides templating for the timing and placement of the acyl and aminoacyl monomers incorporated into the final natural product.

† This work was supported in part by National Institutes of Health Grant AI 42736 to C.T.W.

* To whom correspondence should be addressed. Phone: (617) 432-1715. Fax: (617) 432-0438. E-mail: walsh@walsh.med.harvard.edu.

‡ These authors contributed equally to this work.

[1] Abbreviations: ArCP, aryl carrier protein; CoASH, coenzyme A; DTT, DL-dithiothreitol; HPLC, high-performance liquid chromatography; HPT-COOH, 4,5-dihydro-2-(2-hydroxyphenyl)-4-thiazolecarboxylic acid; HPT-Cys, *N*-{[2-(2-hydroxylphenyl)]-4,5-dihydrothiazole-4-carbonyl}cysteine; HPTT-COOH, 2′-(2-hydroxyphenyl)thiazolyl-2,4-thiazolinyl-4-carboxylic acid; HMWP, high-molecular weight protein; IPTG, isopropyl β-D-thiogalactopyranoside; PCP, peptidyl carrier protein; PCR, polymerase chain reaction; PP_i, pyrophosphate; Ppant, 4′-phosphopantetheine; PPTase, phosphopantetheinyl transferase; Sal, salicylate; SDS−PAGE, SDS−polyacrylamide gel electrophoresis; TCA, trichloroacetic acid; TCEP, tris(2-carboxyethyl)phosphine hydrochloride.

10.1021/bi991574n CCC: $18.00
Published on Web 10/02/1999

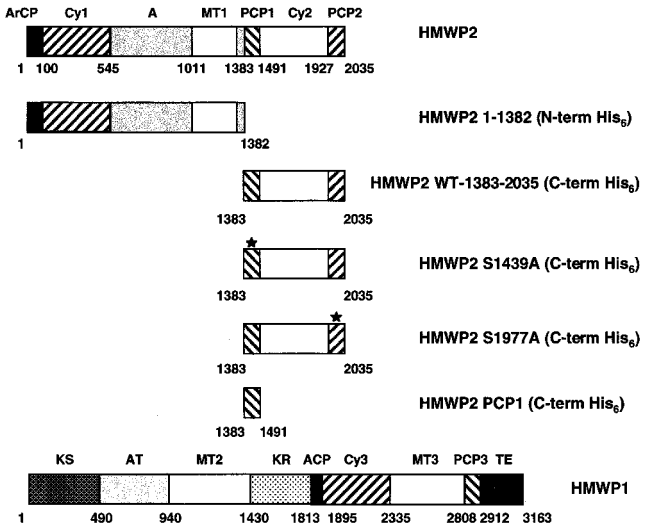

FIGURE 1: Various HMWP2 fragments used for this study and HMWP1. HMWP2 1−1382 was overexpressed and purified as an N-terminal hexahistidine-tagged fusion, while all other fragments were overexpressed and purified as C-terminal hexahistidine-tagged fusions. The star on HMWP2 1383−2035 fragments S1439A and S1977A indicates the position of the mutation. ArCP (residues 1−100), condensation/cyclization domains Cy1 and Cy2 (residues 100−545 and 1491−1927, respectively), the adenylation (A) domain (residues 545−1383), PCP1 (residues 1383−1491), and PCP2 (residues 1927−2035) are indicated above on HMWP2. Although no functional evidence for activity has been shown, residues 1011−1300 have been deemed a potential methyl transferase (MT) domain on the basis of sequence homology. HMWP1 domains KS (β-ketoacyl synthase), AT (acyltransferase), MT2 and MT3 (methyl transferases), KR (β-ketoacyl reductase), ACP (acyl carrier protein), Cy3, PCP3, and TE (thioesterase) are shown above.

Scheme 1

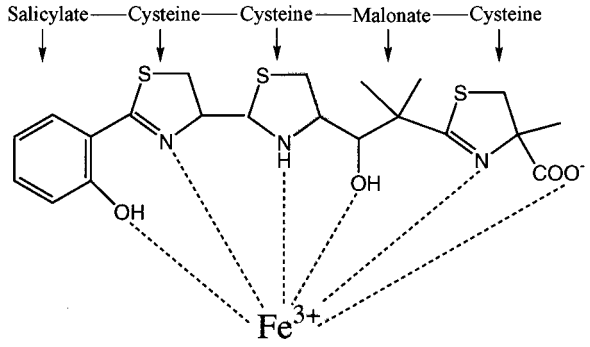

Yersiniabactin-Fe^{3+}, 1

Particularly interesting in both Ybt and other siderophores such as pyochelin (*16*), and in antitumor compounds such as bleomycin (*17*), is the presence of the tandem five-membered ring sulfur heterocycles fused in 4,2-connection, precisely the linkage that would arise from double cyclodehydration of adjacent cysteine-cysteine residues in a precursor molecule (Scheme 1). The 4,2-bisthiazolines could coordinate to metals, as proposed for siderophores, or undergo enzymatic dehydrogenation to the heteroaromatic bithiazole which is a DNA-intercalating and/or minor groove-binding pharmacophore (*17*, *18*). We have noted (*11*, *19*) that the three condensation domains in the two-protein Ybt synthetase, Cy1 and Cy2 in HMWP2 and Cy3 in HMWP1 (Figure 1), are variants of normal NRPS condensation/cyclization (Cy) domains, similar to that found in the thiazoline-forming, first Cy domain of bacitracin synthetase (*20*). Further, we have reported the expression and purification of the 1−1491 fragment of HMWP2 in *Escherichia coli* and validation of its condensation/heterocyclization capacity by catalytic production of hydroxyphenylthiazoline carboxylate (HPT-COO^-) and HPT-cysteine (*19*). In this study, we report the reconstitution of the tandem bisheterocyclization capacity by two fragments (1−1382 and 1383−2035) of HMWP2 in trans that carry out chain translocation and cysteine residue cyclodehydration at both PCP1 and PCP2 thiol waystations and require the Cy1 and Cy2 domains.

MATERIALS AND METHODS

Materials. Salicylic acid, ATP, L-cysteine, DL-dithiothreitol (DTT), Tris, ampicillin, kanamycin, and magnesium chloride were purchased from Sigma Chemical Co. Tris(2-carboxyethyl)phosphine hydrochloride (TCEP) was purchased from Molecular Probes. The *Pfu* DNA polymerase was bought from Stratagene. All DNA oligomers were purchased from Integrated DNA Technologies, Inc. [^{35}S]-L-Cysteine, [^{14}C]-salicylate, [^{3}H]CoASH, and [^{32}P]PP_i were purchased from New England Nuclear. The competent *E. coli* BL21(DE3) cells, the pET vectors, and His·Bind resin were purchased from Novagen, Inc. All restriction enzymes and T4 DNA ligases were purchased from New England Biolabs. Preparation of plasmid DNA, gel purification of DNA fagments, and purification of polymerase chain reaction (PCR)-amplified DNA fragments were performed using the QIAprep spin plasmid miniprep kit, the QIAEX II gel extraction kit, and the QIAquick PCR purification kit, respectively. Ni−NTA superflow resin was purchased from Qiagen. The phosphopantetheinyl transferases *Bacillus subtilis* Sfp (*21*), *E. coli* EntD (*22*), and the carrier protein domain PCP1 (*19*) were purified previously in our laboratory. Plasmids pET22b-irp2/1−1491 (*19*), pET22b-1383−2035 (*22*), and pH6YBTE1 (*19*) which direct expression of the HMWP2 1−1491 fragment, the HMWP2 1383−2035 fragment, and YbtE, respectively, were cloned previously.

Cloning of HMWP2 Fragments. (a) Cloning of the HMWP2 1−1382 Fragment. The *Y. pestis irp2* gene fragment corresponding to HMWP2 residues 1−1382 was cloned into pET28b in two steps. First, a stop codon was introduced just after the codon of residue 1382 by PCR using the *Pfu* polymerase, pET22b-irp2/1−1491 (*19*) as the template, and primers 1320for and 1382rev (Table 1). This PCR product was cloned into the *Not*I−*Xho*I sites of pET22b-irp2/1−1491 to give pET22b-irp2/1−1382. The 4153 bp fragment corresponding to residues 1−1382 of HMWP2 was extracted and ligated into the *Nde*I−*Xho*I sites of the pET28b vector to give pET28b-irp2/1−1382. The resulting plasmid directs production of the 1−1382 fragment as a histidine tag fusion with the amino acid sequence MGSSHHHHHHSSGLVPRG-SH appended to the N-terminus. The DNA sequence of the pET28b-irp2/1−1382 insert was confirmed by sequencing (Dana Farber Molecular Biology Core Facility).

(b) Cloning of Mutants S1977A and S1439A of the HMWP2 1383−2035 Fragment. The site-directed mutants, S1977A and S1439A, on the *Y. pestis irp2* 1383−2035 fragment were constructed using the SOE (splicing by overlap extension) method (*24*). In the first round of PCR, the sequence upstream and downstream of the mutation was

Table 1: Sequence of DNA Primers

primer	restriction site	primer sequence[a] (5′ → 3′)
1320for	*Not*I	CATTATTTAGCGCGGCCGCCTTCAA
1382rev	*Xho*I	GCGCCTCTCGAGTTATTTTCCCGTTAGCGCTCAG
Irp1383.for	*Nde*I	GAATTCCATATGATTGACTACCAGGCGCTGA
Irp2035.rev	*Xho*I	TGACCGCTCGAGTATCCGCCGCTGACGACGG
S1439A.for		CGGCGAT**GC**CCTGCTGGCGACCCGTCT
S1439A.rev		AGACGGGTCGCCAGCAGG**GC**ATCGCCG
S1977A.for		AGGCAGGCGCAACG**G**CGCTGAATCTG
S1977A.rev		CCAGATTCAGCG**C**CGTTGCGCCTGCCTC

[a] Restriction sites are underlined, and the mutation sites are bold.

amplified separately using pIRP2 (*5*), the primer pairs (Table 1) 1383.fwd/S1439A.rev and S1439A.fwd/2035.rev for S1439A and 1383.fwd/S1977A.rev and S1977A.fwd/2035.rev for S1977A, and *Pfu* polymerase. After the PCR-amplified DNA fragments had been gel purified, the second round of PCR was carried out using the primer pair 1383.for/2035. The purified SOE-amplified DNA fragments S1439A and S1977A were digested with *Nde*I−*Bsu*361 and *Bsu*361−*Xho*I, respectively, and subcloned into pET22b-1383−2035 to give plasmids pET22b-S1439A and pET22b-S1977A, respectively. The insert sequences were confirmed by DNA sequencing. These plasmids direct overproduction of the wild-type PCP1−Cy2−PCP2 fragment and its two mutants containing their respective mutations as hexahistidine tag fusions with the amino acid sequence LEHHHHHH at the C-terminus.

Overproduction and Purification of YbtE and HMWP2 Fragments. Cultures of *E. coli* strain BL21(DE3) transformed separately with pH6YBTE1, pET22b-1383−2035, pET22b-S1439A, pET22b-S1977A, pET28b-irp2/1−1382, and pET22b-irp2/1−1491 [4 L, 2YT media, 100 μg/mL ampicillin (except pET28b-irp2/1−1382 for which 50 μg/mL kanamycin was used)] were grown at 30 °C to an optical density (600 nm) of 0.8 and then induced with 1 mM isopropyl β-D-thiogalactopyranoside (IPTG) and incubated at 22 °C. Cells were harvested for the YbtE, 1383−2035, S1439A, and S1977A after 4 h, and the cell paste was resuspended in buffer A [20 mM Tris-HCl (pH 7.9) and 0.5 M NaCl]. For HMWP2 1−1382 and 1−1491, cells were harvested after the optical density (600 nm) reached 1.9 and the cell pellets were resuspended in buffer A with 2 mM imidazole. Cells were lysed by passing them twice through a French pressure cell at 15 000 psi, and the lysate was clarified by centrifugation (35000*g*) for 30 min. YbtE, HMWP2 1383−2035, HMWP2 S1439A, and S1977A proteins were purified from the lysate by nickel chelate chromatography over His·Bind resin (5 mL column) according to the manufacturer's specifications (Novagen). Fractions containing protein were identified by SDS−polyacrylamide gel electrophoresis (SDS−PAGE) and then pooled, dialyzed against 50 mM Tris-HCl (pH 8.0), 2 mM DTT, and 5% glycerol. HMWP2 1−1382 and HMWP2 1−1491 proteins were purified from the lysate by nickel affinity chromatography with Ni−NTA superflow resin using batch purification (Qiagen). The protein-containing fractions were pooled and dialyzed against a storage buffer containing 50 mM Tris-HCl (pH 8.0), 0.5 mM TCEP, 10 mM $MgCl_2$, 0.1 mM EDTA, and 10% glycerol. All proteins were flash-frozen in liquid nitrogen and stored at −80 °C. Concentrations of the purified proteins were determined spectrophotometrically at 280 nm using the calculated extinction coefficients 54 420, 105 840, 266 460, and 258 210 M^{-1} cm^{-1} for YbtE, HMWP2 1383−2035 constructs, HMWP2 1−1491, and HMWP2 1−1382, respectively.

Assay for the Phosphopantetheinylation of PCP Domains. A tricholoracetic acid (TCA) precipitation radioassay which is used to measure the phosphopantetheinyl transferase activity as the extent of covalent attachment of [^{3}H]Ppant from [^{3}H]CoASH to the carrier protein substrate was performed as described previously (*23*, *25*).

Autoradiography Demonstrating the Aminoacylation of HMWP2 Fragments with [^{35}S]-L-Cysteine. For autoradiography, HMWP2 1−1382 (1 μM) was incubated at room temperature for 20 min with Sfp (0.13 μM), CoA (1 mM), salicylate (1 mM), TCEP (5 mM), $MgCl_2$ (10 mM), Tris-HCl (75 mM, pH 8.8), ATP (10 mM) (except where indicated), and one of the HMWP2 fragments (PCP1, S1439A, S1977A, or wild-type 1383−2035) (15 μM). [^{35}S]-L-Cysteine (0.68 mM, 55.5 Ci/mol) was then added to each reaction mixture, and the mixtures were incubated at 30 °C for 20 min. For loading onto a 4 to 20% Tris-glycine gradient gel (Bio-Rad), 25 μL of each reaction mixture was mixed with SDS sample buffer (without reducing agent). For visualization, the gel was stained with Coomassie blue solution, destained, and soaked in Amplify (Amersham) for 15 min. The dried gel was exposed to film for 5 days.

Assay for the ATP−[^{32}P]PP_i Exchange Reaction. The ATP−pyrophosphate (PP_i) exchange reaction was performed as described previously (*26*) with minor modifications. A reaction mixture (final volume of 100 μL, duplicate) containing 75 mM Tris-HCl (pH 8.8), 10 mM $MgCl_2$, 5 mM TCEP, 1 mM sodium [^{32}P]PP_i (4 Ci/mol), ATP, L-cysteine, and 30 nM HMWP2 1−1382 was incubated for 5 min at 37 °C. The reaction was stopped by the addition of 0.5 mL of a charcoal suspension [1.6% (w/v) activated charcoal, 0.1 M tetrasodium pyrophosphate, and 0.35 M perchloric acid]. The charcoal was pelleted by centrifugation for 5 min at 16060*g*. The liquid was removed, and the charcoal pellet was washed twice with 0.9 mL of buffer containing 0.1 M tetrasodium pyrophosphate and 0.35 M perchloric acid. The pellet was resuspended in 0.5 mL of water and added to 7 mL of scintillation fluid (Ultima Gold, Packard); [^{32}P]ATP was quantitated by liquid scintillation counting. For the determination of the ATP K_M, varying concentrations of ATP were utilized with L-cysteine at 10 mM. For the L-cysteine K_M determination, the ATP concentration was constant at 10 mM.

Detection, Identification, and Kinetic Studies of Intermediates Synthesized by YbtE and Different Combinations of Fragments of HMWP2 in Vitro. Time Courses of Acyl−Cys

Intermediate Formation at 30 °C Catalyzed Separately by HMWP2 1−1382, 1−1382/PCP1, 1−1491, 1−1382/1383−2035, and 1−1382/S1977A. The reactions were carried out as described previously (*19*) with some modifications. The fragments of HMWP2 were incubated with 75 mM Tris-HCl (pH 8.8), 10 mM $MgCl_2$, 2.5 mM TCEP, 0.13 μM Sfp, 1 mM CoASH, 0.5 μM YbtE, 5 mM L-cysteine, 1 mM salicylate, and 10 mM ATP (without ATP in the control reaction). Prior to addition of ATP, the mixture was incubated at 30 °C for 20 min to allow phosphopantetheinylation of fragments of HMWP2 by Sfp. After addition of ATP, the reaction mixture (500 μL) was incubated at 30 °C and 50 μL samples were removed at various times. (The volume of each sample for the time course of wild-type 1−1382/1383−2035 is 100 μL.) Each 50 μL sample was acidified by addition of 10 μL of 8.5% phosphoric acid. The acidified mixture (pH ≈1.5) was extracted by 1 mL of ethyl acetate. A portion of the organic layer (900 μL) was dried in a SpeedVac. The dried residue was dissolved in 200 μL of 30% acetonitrile/water. Most of the solution (180 μL) was analyzed by HPLC (Beckman) connected to a C18 reverse phase column (VYDAC, 250 mm × 4.6 mm) with a detector wavelength of 254 nm and a mobile phase with the following gradient. Mobile phase A was a mixture of formic acid (0.1 mL) and triethylamine (0.2 mL) in water (1 L) (pH 3.3). Mobile phase B was a 4:1 mixture of acetonitrile and mobile phase A. At a flow rate of 1 mL/min, the gradient was as follows: time 0.0 min, 10% B; 23.0 min, 100% B; 23.1 min, 10% B; and at 1.5 mL/min, time 25.0 min (10% B), and at 1 mL/min.

Time Course of Sal-Cys Formation at 37 °C Catalyzed by YbtE (10 μM) Alone. The reactions were performed in a manner similar to that described above in the absence of Sfp, CoA, and thereby phosphopantetheinylation. The reaction products were analyzed in the same manner as described above.

Measurement of K_M Values of 1−1382/S1977A, 1−1382/PCP1, and Wild-Type 1−1382/1383−2035 at 30 °C. For the determination of K_M values, varying concentrations of S1977A, PCP1, or wild-type 1383−2035 were used while the 1−1382 concentration was held at 3 μM. The reactions were performed in a manner similar to that described for the acyl-Cys formation except that the volume of each reaction was 100 μL, and the reaction time was 140 min. The reaction mixtures were analyzed as described above.

Measurement of the Velocity for Acyl-Cys Intermediate Formation at 30 °C in the Presence of DTT. The reactions and product analysis were conducted in the same manner as described above for acyl-Cys formation. Reaction mixtures (100 μL), including 1−1491 (0.5 μM) or 1−1382 (1 μM), 75 mM Tris-HCl (pH 8.8), 10 mM $MgCl_2$, 2.5 mM TCEP, 0.13 μM Sfp, 1 mM CoASH, 0.5 μM YbtE, 5 mM L-cysteine, 1 mM salicylate, 10 mM ATP, and 0−150 mM DTT, were incubated at 30 °C for 60 min.

Isolation and Identification of Products Synthesized by 1−1382, 1−1491, and Wild-Type 1−1382/1383−2035 for Mass Spectrometry Analysis. A solution (1000 μL) of 5 μM 1−1382, 5 μM wild-type 1383−2035, 0.13 μM Sfp, 0.5 μM YbtE, 75 mM Tris-HCl (pH 8.8), 10 mM $MgCl_2$, 2.5 mM TCEP, 1 mM CoASH, 5 mM L-cysteine, 1 mM salicylate, and 10 mM ATP was incubated at 30 °C for 12 h. The reaction was quenched with 200 μL of 8.5% phosphoric acid. The acidified mixture was extracted with 1 mL of ethyl acetate four times. The organic layer was combined in a glass vial and divided into 0.8 and 4.2 mL portions, and then dried separately under reduced pressure. The dried residue from the 0.8 mL portion was submitted directly for LC−MS positive ion trap mass spectrometry analysis (Biopolymer Facility, Harvard Medical School). The individual products were purified from the 4.2 mL portion using the same HPLC conditions as described above for acyl-Cys formation. The dried residues were submitted to LC−MS analysis. The reactions catalyzed by 1−1382 and 1−1491 separately were conducted in a manner similar to that described above except that there was 250 mM DTT in the reaction mixture (200 μL). The reaction products were extracted, dried, and analyzed by LC−MS.

To further confirm the identity of the products synthesized by wild-type 1−1382/1383−2035, L-cysteine(3,3-D_2) (Cambridge Isotope Laboratory, Cambridge, MA) was used as the cysteine substrate in a 200 μL reaction mixture. The reaction products were extracted, dried, and analyzed by LC−MS.

HPLC Calibration of Three Synthetic Standard Compounds. Known quantities of synthetic Sal-Cys, HPT-Cys, and HPTT-COOH standards (*19*) were injected and analyzed separately by HPLC in the same manner as described above for acyl-Cys formation. From the integrated area (A) of HPLC peaks and the corresponding amount of standard compounds, the standard calculation curves for Sal-Cys, HPT-Cys, and HPT-COOH were determined to be $(4.8400 \times 10^{-6})A$, $(1.5716 \times 10^{-6})A$, and $(4.2751 \times 10^{-6})A$ nmol, respectively.

Product Quantitation. Each peak of HPLC traces was integrated by computer to obtain its peak area. The integrated area was converted into quantity using the above corresponding standard calculation curve. Due to the lack of synthetic standards, the HPT-Cys-Cys and HPTT-Cys peaks were estimated using the HPT-Cys and HPTT-COOH standard curves, respectively.

Data Analysis. For the HPLC time courses, the data were fitted to the linear equation [product] = $k_{obs}E_0t$, where E_0 represents the enzyme concentration and k_{obs} the observed steady-state rate. For the Sal-Cys formation catalyzed by YbtE alone, the data were fitted to the single-exponential equation [product] = $E[1 - \exp(k_{obs}t)]$, where E represents the active enzyme concentration and k_{obs} the observed single-turnover rate. For the measurement of K_M of 1−1382/S1977A, 1−1382/PCP1, and wild-type 1−1382/1383−2035, the data were fitted to the Michaelis−Menten equation [product] = $E_0Sk_{cat}/(K_M + S)$, where E_0 represents the constant concentration of 1−1382, k_{obs} the maximum steady-state turnover number, and S the concentrations of S1977A, PCP1, and wild-type 1383−2035. [product] for the K_M measurements of both 1−1382/S1977A and 1−1382/PCP1 is the concentration of HPT-Cys, while [product] for the K_M of wild-type 1−1382/1383−2035 represents the total amount of HPT-Cys, HPT-COOH, HPT-Cys-Cys, HPTT-Cys, and HPTT-COOH. Data from the measurement of velocity for acyl-Cys formation in the presence of DTT were fitted to the equation [product] = k_1[DTT]/[[DTT] + $K_{M,DTT}$ + ($K_{M,DTT}/K_{M,Cys}$)[Cys]] + k_2[Cys]/[[Cys] + $K_{M,Cys}$ + ($K_{M,Cys}/K_{M,DTT}$)[DTT]] ≈ k_1[DTT]/([DTT] + $K_{M,DTT}$) + C, where k_1 and k_2 represent the rates of intermediate cleavage by DTT and cysteine, respectively, $K_{M,DTT}$ and $K_{M,Cys}$ are the apparent

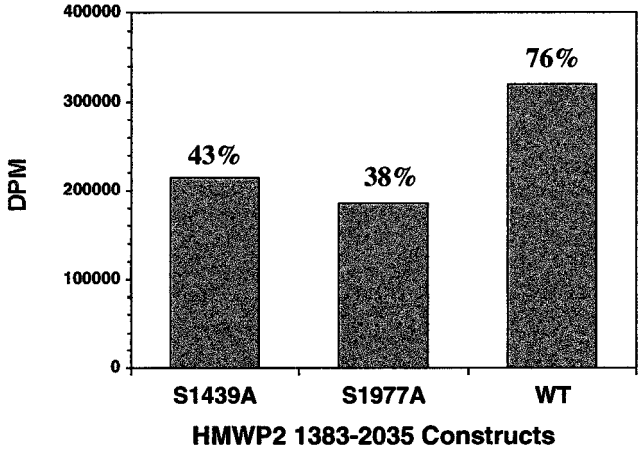

FIGURE 2: Stoichiometry of the phosphopantetheinylation of apo-HMWP2 fragments S1439A, S1977A, and wild-type 1383−2035 that is dependent on *E. coli* EntD. All reaction mixtures contained [^{3}H]CoASH (150 μM, 192 Ci/mol) and EntD (800 nM). In the absence of EntD, 0.4% radioactivity incorporation was observed (data not shown). Percentages were based upon the calculated radioactivity expected for stoichiometric modification (100%) of the two apo PCP domains in the wild-type fragment or of one (50%) apo PCP domain in each mutant.

K_M constants for DTT and cysteine, respectively, and C is the intermediate formation rate in the absence of DTT.

RESULTS

Overproduction and Characterization of Ybt HMWP2 Fragments 1−1382 and 1383−2035

As depicted in Figure 1, the HMWP2 subunit (2035-amino acid) of HMWP2 is proposed to contain six functional domains, three of which are carrier protein domains (ArCP, PCP1, and PCP2) that will undergo posttranslational phosphopantetheinylation and ultimately serve as thiol waystations for acylation by salicylate (ArCP) and cysteine (PCP1 and PCP2). There is one adenylation (A) domain (residues 545−1382), and there are two condensation/cyclization domains, Cy1 (100−544) and Cy2 (1491−1927). Our previous success (*19*) in overproducing the 1−1491 fragment allowed validation of the function of the ArCP and PCP1 carrier protein domains, the cysteine-selective adenylation domain, and the Cy1 domain (for both amide formation and cyclodehydration of the growing acyl chain).

To evaluate the potential for tandem 4,2-bisheterocyclization of adjacent Cys-Cys residues to the bisthiazoline during chain growth, we have now focused on the three-domain fragment PCP1−Cy2−PCP2, spanning the 653 C-terminal residues, 1383−2035, of HMWP2. In principle, this 75 kDa fragment, once doubly phosphopantetheinylated, could be capable of undergoing aminoacylation by cysteine on each Ppant-SH, followed by condensation and cyclodehydration mediated by Cy2. The cysteine would have to be activated in trans by the adenylation domain. Although small fragments of HMWP2 that should encompass the adenylation domain (545−1382) were inactive, the 1−1382 157 kDa fragment turned out to be useful. Therefore, HMWP2 1−1382 (as an N-terminal His_6 fusion) and HMWP2 1383−2035 (as a C-terminal His_6 fusion) (Figure 1) were constructed, overproduced, and purified to substantial homogeneity (Figure 3A).

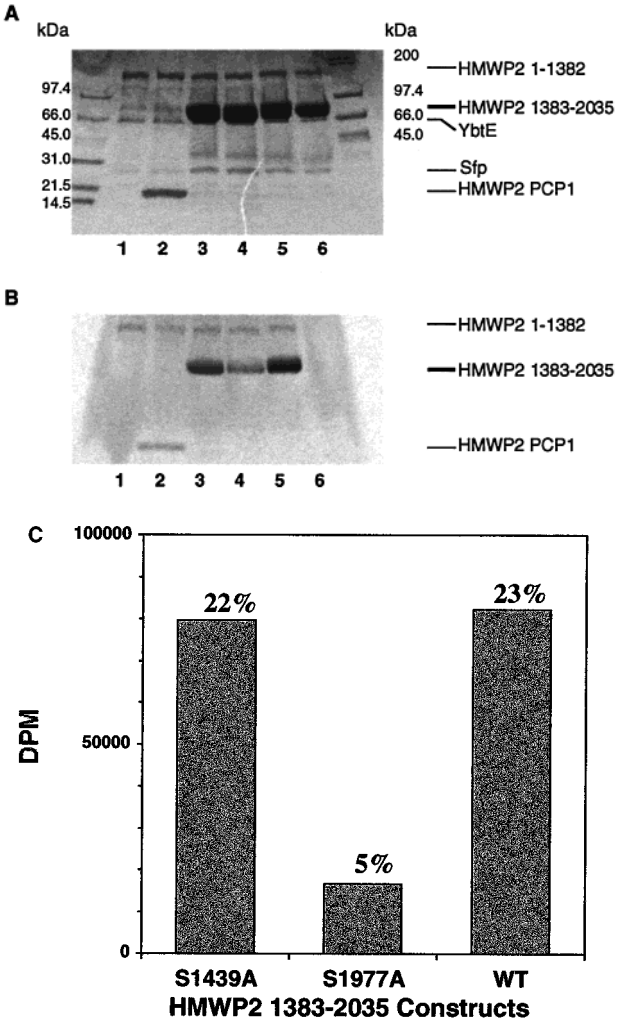

FIGURE 3: Demonstration of the covalent loading of the HMWP2 fragments with [^{35}S]-L-cysteine. (A) Coomassie-stained gel (4 to 20%) of reaction mixtures. (B) Autoradiograph of this gel. All reaction mixtures contained [^{35}S]-L-cysteine (0.68 mM, 55.5 Ci/mol), Sfp (0.13 μM), CoA (1 mM), TCEP (5 mM), $MgCl_2$ (10 mM), Tris-HCl (75 mM, pH 8.8), and ATP (10 mM) except where indicated: lane 1, HMWP2 1−1382 (1 μM); lane 2, PCP1 (15 μM) and HMWP2 1−1382 (1 μM); lane 3, S1439A (15 μM) and HMWP2 1−1382 (1 μM); lane 4, S1977A (15 μM) and HMWP2 1−1382 (1 μM); lane 5, HMWP2 wild-type 1383−2035 (15 μM) and HMWP2 1−1382 (1 μM); and lane 6, HMWP2 wild-type 1383−2035 (15 μM) and HMWP2 1−1382 (1 μM), without ATP. (C) Bar graph demonstrating the stoichiometry of covalent loading of HMWP2 fragments (20 μM) with [^{35}S]-L-cysteine (0.68 mM, 55.5 Ci/mol). In the absence of ATP, 0.9% radioactivity incorporation was noted (data not shown). Percentages were based upon the total radioactivity expected for 100% aminoacylation of the two holo PCP domains of HMWP2 wild-type 1383−2035.

First, the partial reactions characteristic of each fragment were demonstrated to assess functionality of specific domains. The three-domain 1−1382 (ArCP−Cy1−A) shows the anticipated cysteine-dependent [^{32}P]PP_i−ATP exchange with K_M values of 1.6 and 2.3 mM for L-Cys and ATP, respectively, and an average k_{cat} of 93 min^{-1}, compared to the values of 0.65 and 0.36 mM and 440 min^{-1} seen with the 1−1491 fragment (*19*), indicative of reversible formation of Cys-AMP. The Ser52 in the ArCP domain could be posttranslationally primed with cosubstrate CoASH via the broad specificity phosphopantetheinyl transferase (PPTase) Sfp from *B. subtilis* (*21*). Sfp was utilized because the Ybt-

Table 2: Product Release Rates at 30 °C

enzyme	Sal-Cys (min^{-1})	HPT-Cys (min^{-1})	HPT-Cys-Cys (min^{-1})	HPTT-Cys and HPTT-COOH (min^{-1})
YbtE[a]	0.0021 ± 0.0005			
1−1382	0.033 ± 0.001			
1−1491		0.087 ± 0.006		
1−1382/1383−2035		0.057 ± 0.001	0.035 ± 0.002	0.033 ± 0.001
1−1382/S1977A		0.17 ± 0.01		
1−1382/PCP1		0.043 ± 0.005		

[a] The reaction rate was measured at 37 °C.

dedicated *Y. pestis* PPTase has yet to be identified. The Ppant moiety in holo 1−1382 could then be acylated to form the salicyl-S-ArCP moiety with salicylate, ATP, and the salicyl-AMP ligase YbtE (data not shown).

Sfp likewise served to prime both Ser1439 (PCP1) and Ser1977 (PCP2) to convert the bis apo form of 1383−2035 into the bis holo form. Covalent phosphopantetheinylation of the three sites on the two fragments could be readily assessed using [^{3}H]CoASH, SDS−PAGE, and autoradiography (*23*, *25*).

To confirm that both PCP1 and PCP2 could be converted to the Ppant holo forms, the two single mutants S1439A and S1977A of the wild-type HMWP2 1383−2035 fragment (Figure 2) were analyzed. Each mutant was labeled with [^{3}H]-Ppant to about half the extent of wild-type 1383−2035 which is consistent with a 1:1 stoichiometry of priming of both PCP1 and PCP2 in the wild-type 1383−2035 fragment. When the holo forms of 1−1382/1383−2035 and 1−1382/PCP1 were mixed, the PCP1−Cy2−PCP2 and PCP1 fragments were covalently labeled with [^{35}S]-L-cysteine in reactions dependent on ATP (Figure 3). Both the PCP1 mutant (S1439A) and the PCP2 mutant (S1977A) in their mono Ppant-modified holo forms were also labeled with [^{35}S]-cysteine after denaturing gel electrophoresis (Figure 3), confirming cysteinyl transfer by the adenylation domain to each thiol waystation. This result shows that the cysteinylation of PCP2 by the adenylation domain upstream can be direct and need not come by obligate aminoacylation at PCP1 and subsequent transthiolation. In fact, the holo PCP2 domain was a better substrate than the holo PCP1 domain for cysteinylation in trans as judged by the stoichiometry of cysteine incorporation, 5% at PCP1 and 22% at PCP2 (Figure 3C). Thus, the PCP1 domain may be more labile than PCP2 in this three-domain fragment. At this point, the two holo forms of the 157 and 75 kDa fragments of HMWP2 were analyzed for functional reconstitution.

Evaluation of Catalytic Function of HMWP2 1−1382 with Partner Fragments

YbtE Alone. Our previous results have demonstrated that YbtE is a salicyl-AMP ligase capable of covalent acylation of the holo ArCP domain of HMWP2 (*19*), most likely through the following steps:

$$\text{YbtE} + \text{ATP} + \text{salicylate} = \text{PP}_\text{i} + \text{YbtE·salicyl-AMP}$$

$$\text{YbtE·salicyl-AMP} + \text{ArCP} \rightarrow \text{YbtE} + \text{ArCP-Sal}$$

We evaluated whether YbtE could produce Sal-Cys, **2**, by direct capture of Sal-AMP by cysteine, and a small peak of **2** was detected in HPLC traces from incubations of ATP, salicylate, L-cysteine, and YbtE (10 μM). The observed rate (data not shown) of Sal-Cys formation at 37 °C was 0.0021 min^{-1} (half-time of 330 min) shown in Table 2. Since the ATP−[^{32}P]PP$_i$ isotope exchange assay indicates reversible formation of Sal-AMP occurs at 250 min^{-1} (*19*), the thiolysis step to form **2** must be rate-limiting. This thiolysis by cysteine is more than 4 orders of magnitude slower than the thiolysis by the holo-ArCP domain on the reaction path (94 min^{-1}; *19*) and thus kinetically incompetent to reroute much flux. As will be noted below, the observed Sal-Cys in reactions with 1−1382 with or without 1383−2035 comes largely from thiolysis of the Sal-S-ArCP intermediate, especially at lower temperatures (30 °C) and the low concentrations of YbtE (0.25−0.5 μM) used in incubations.

1−1382 Alone. When catalytic turnover was assessed for holo 1−1382 on its own, without the bis-holo 1383−2035 in the presence of ATP, cysteine, salicylate, and YbtE by HPLC analysis, the patterns displayed in Figure 4 were obtained. No product was released in the absence of ATP. On addition of ATP, there was a time-dependent accumulation of a peak that cochromatographed with authentic Sal-Cys, **2**, which was produced at a rate of 0.033 min^{-1} (Table 2). Given that 1−1382 lacks PCP1 and PCP2 (see Figure 1), the two domains that covalently tether cysteine, it seemed likely that the Sal-Cys arose from adventitious capture of Sal-S-ArCP by the thiolate of cysteine reacting from solution, a facile transthiolation from one acyl thioester to form another, salicyl-S-cysteine. This step would be followed by a rapid and favorable S to N acyl shift of the salicyl group which forms the hydrolytically stable, observed salicyl-N-cysteine, **2** (Scheme 2). Other thiols should also compete; DTT was particularly effective (see below), but the sal-S-DTT (not detected) will eventually hydrolyze. As a matter of routine assay, the DTT used previously in protein isolation buffers for enzyme stability (*19*) was replaced with the phosphine reducing agent TCEP (*27*) to permit detection of the Sal-S-ArCP and other, more downstream acyl-S-enzyme intermediates (see below) that could be captured by cysteine.

1−1382 plus 1383−2035. When the bis holo HMWP2 1383−2035 fragment was added to holo 1−1382 incubations to provide all 2035 residues of HMWP2 in two fragments in trans, the rate of Sal-Cys release dropped by about 50% and three new peaks, representing compounds **3**−**5** (Scheme 3), were detected on HPLC analysis (Figure 5). These peaks were detected with TCEP as the reducing agent (trace b), but not when DTT was present (trace a). DTT presumably competes with the thiolate side chain of the cysteinylated S-PCP1 for the translocating acyl chains. One of the HPLC-detectable products was identified by HPLC and LC−MS analysis ($[M + H]^+ = 327$) (Table 3) as the monothiazoline hydroxyphenylthiazoline-cysteine (HPT-Cys), **3**, previously detected in catalytic release by the HMWP2 1−1491

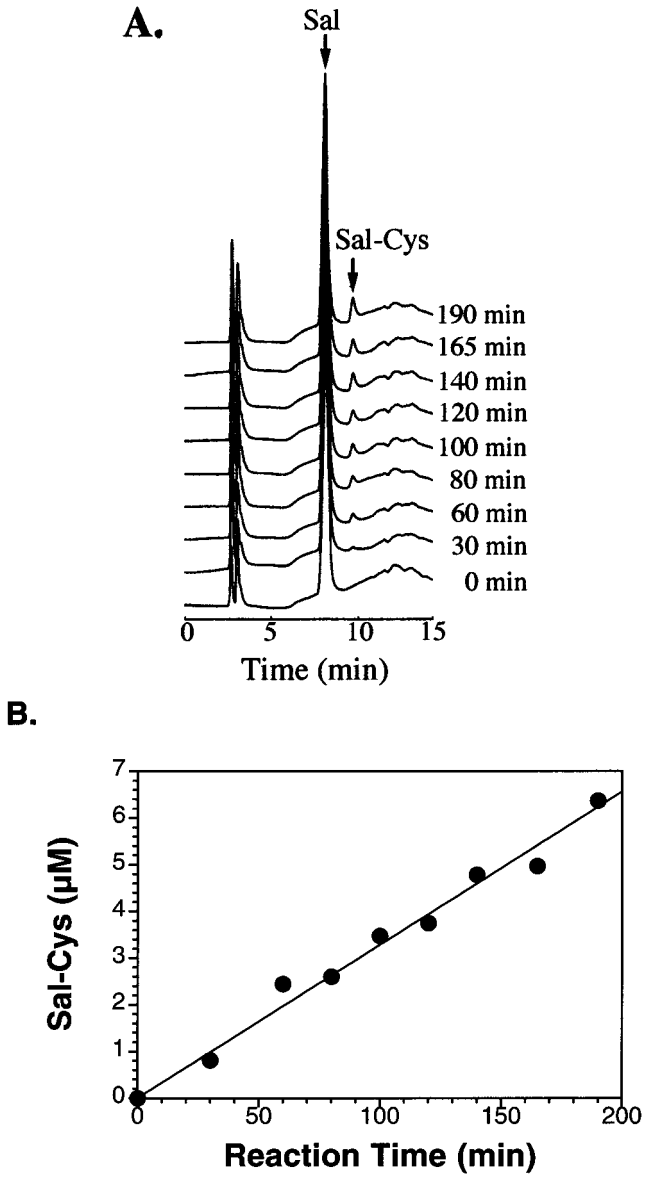

FIGURE 4: Time course of Sal-Cys formation catalyzed by 1−1382 (1 μM) at 30 °C in the presence of TCEP (2.5 mM), YbtE (0.25 μM), and the substrates L-cysteine (5 mM), salicylate (1 mM), and ATP (10 mM). (A) HPLC traces. The only product at 9.7 min was identified as Sal-Cys by both co-injection with a synthetic standard and high-resolution LC−MS. The major peak at 8.1 min represents salicylate. (B) Plot showing the linearity of the concentration of Sal-Cys (●) vs reaction time. From the solid line, a k_{obs} of 0.033 min^{-1} is calculated.

fragment (*19*). A second, new product had the mass anticipated for HPT-Cys-Cys, **4** (Table 3), and is presumed to be the thiolysis product from capture of an HPT-Cys-S-enzyme species. A transient HPT-Cys-S-Cys thioester would undergo the intramolecular S to N acyl shift to yield **4**. The third product that could be detected on HPLC had the expected $[M + H]^+$ ion at 410 for hydroxyphenyl-thiazole-thiazoline-cysteine (HPTT-Cys), **5**, in LC−MS analysis (Table 3). This is a tandem 4,2-bisheterocyclic product, presumably reflecting thiolysis by cysteine in solution of an HPTT-S-enzyme intermediate. We note that the five-membered ring heterocycle conjugated to the hydroxyphenyl group has been oxidized to the heteroaromatic thiazole, rather than the anticipated dihydrothiazoline ring. In our efforts to synthesize an authentic sample of hydroxyphenyl-thiazolinyl-

Scheme 2

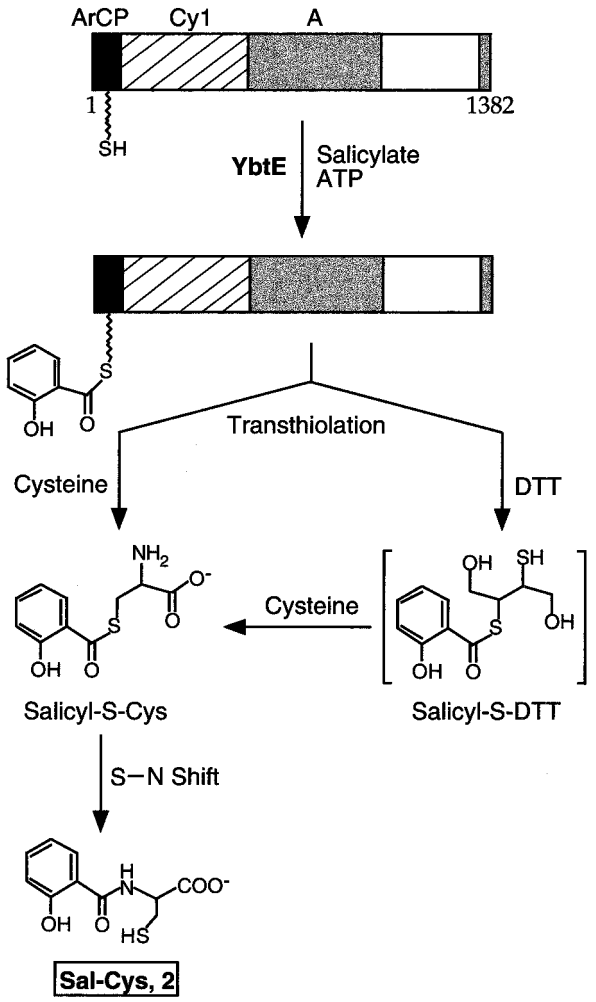

thiazoline acid and the corresponding bisthiazolinyl-amide to cysteine, we obtained only the product with the first sulfur heterocycle oxidized to the thiazole (*19*). We have surmised this is due to facile autoxidation to produce the conjugated, planar hydroxyphenyl-thiazole moiety (*19*) and expect this has also happened in the workup of the enzymatic incubations with the fragments of HMWP2 described here. Moreover, minor amounts of three additional products could be detected and separated by HPLC (data not shown) and mass spectra obtained (Scheme 3, compounds **6**−**8**). These compounds had the molecular weight values expected for Sal-Cys-Cys, **6** ($[M + H]^+ = 345$), HPT-COOH, **7** ($[M + H]^+ = 224$), and HPTT-COOH, **8** ($[M + H]^+ = 307$, oxidized as HPTT-Cys) (see Table 3). **7** and **8** would be hydrolysis products from the same HPT-S-PCP1 and HPTT-S-PCP2 acyl enzyme intermediates that, on competing thiolysis, yield **3** and **5**, respectively. Sal-Cys-Cys would be the thiolysis product expected if a small amount of Sal-Cys-S-enzyme species was captured before cyclization to the HPT-S-enzyme. Sal-Cys, **2**, was the expected thiolysis product from Sal-S-ArCP as with 1−1382 alone.

Confirmation of the identity and content of cysteine equivalents in products **2**−**8** was obtained by conducting similar incubations with L-cysteine(3,3-D_2) in place of L-cysteine. As shown in Table 3, the Sal-Cys peak increased by 2 mass units and the Sal-Cys-Cys by 4 mass units as anticipated. Analogously, the HPT-Cys mass went from 327

Scheme 3

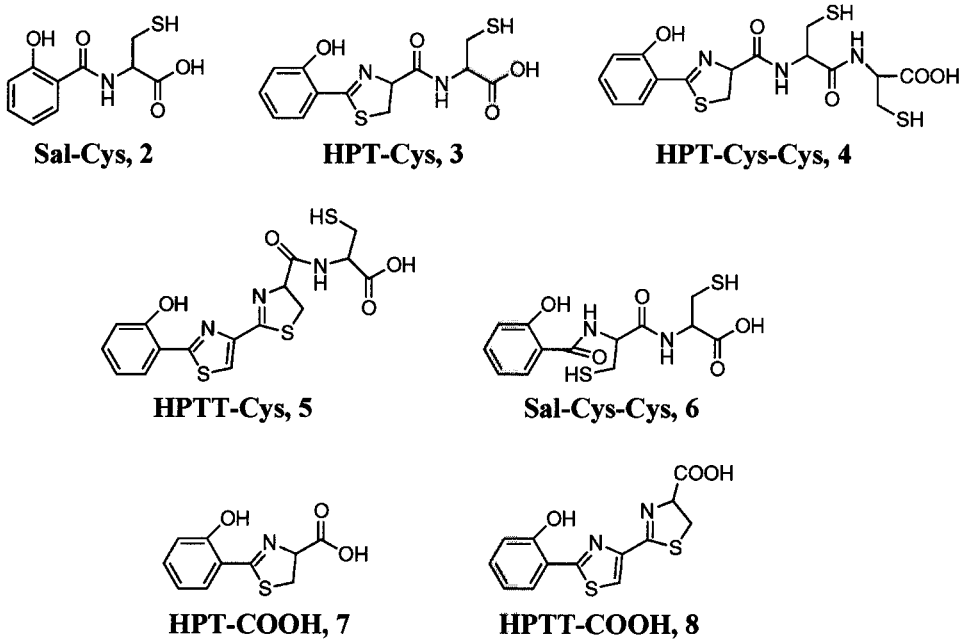

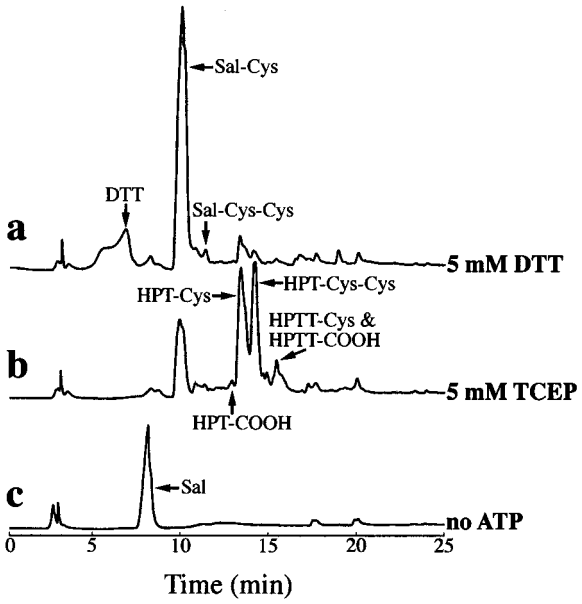

FIGURE 5: DTT effect on the formation of acyl-Cys intermediates catalyzed by wild-type 1−1382 and 1383−2035 in trans. A solution of 1−1382 (5 μM) and 1383−2035 (5 μM) was incubated with YbtE (0.5 μM), Sfp (0.1 μM), CoA (1 mM), L-cysteine (5 mM), salicylate (1 mM), ATP (10 mM), $MgCl_2$ (10 mM), and Tris-HCl (75 mM, pH 8.8) for 10 h at 30 °C. The reaction was quenched, and the products were extracted and analyzed by HPLC. The differences in the components of the three reactions are as follows: (a) 5 mM DTT, (b) 5 mM TCEP, and (c) no ATP and 5 mM TCEP.

to 331 and the HPT-Cys-Cys mass from 430 to 436, reflecting two and three dideuteriocysteine units incorporated into **3** and **5**, respectively. The HPTT-COOH and HPTT-Cys should have two and three cysteine equivalents, respectively, but have lost one of the deuterium atoms on oxidation of the thiazoline to thiazole, for an anticipated gain of the five mass units in the L-cysteine(3,3-D_2) incubations, consistent with the observed mass change of three units, or from 307 to 310 (HPTT-COOH) and from 410 to 415 (HPTT-Cys).

Table 3: Mass Spectra Data ($[M + H]^+$ Values) of Enzymatic Products of the HMWP2 Wild-Type 1−1382/Wild-Type 1383−2035 Reaction in the Presence of either L-Cysteine or L-Cysteine(3,3-D_2)

compound	calculated weight	observed weight	observed weight [L-Cys(3,3-D_2)]
Sal-Cys	242.04	242.06	244.06
Sal-Cys-Cys	345.05	344.89	348.98
HPT-COOH	224.03	224.38	226.38
HPT-Cys	327.04	327.20	331.23
HPT-Cys-Cys	430.05	430.23	436.19
HPTT-COOH	309.03	307.17	310.14
HPTT-Cys	412.04	410.20	415.34

Time course analysis of the rates of formation of HPT-Cys (**3**), HPT-Cys-Cys (**4**), and HPTT-Cys/HPTT-COOH (**5** and **8**) catalyzed by 1−1382/1383−2035 (5 μM each) at 30 °C was performed, showing that the longer the reaction time, the larger the product peaks (Figure 6A). On the basis of the K_M of 20 μM for 1−1382/S1977A, the active concentration of the 1−1382/1383−2035 complex was estimated to be 0.86 μM of the total concentration of 5 μM. The release rates for **3**, **4**, and **5** and **8** were calculated (Figure 6B) to be 0.057, 0.035, and 0.033 min^{-1}, respectively (Table 2). The total flux sums to 0.125 min^{-1}. While slow, these rates reflect multiple catalytic turnovers during the 180 min reaction.

1−1382 plus PCP1 and S1439A or S1977A Mutants of 1383−2035. The three-domain PCP1−Cy2−PCP2 1383−2035 fragment has two peptidyl carrier protein domains. To probe directionality and regioselectivity of salicyl and cysteinyl growing chain transfers, the two single mutants S1439A (PCP1) and S1977A (PCP2) were assayed in in trans reconstitutions with holo 1−1382. The Ser to Ala mutants ensure that when phosphopantetheinyl priming is carried out by the Sfp PPTase, only one Ppant group can be introduced, with regioselective control. Each of the S1439A and S1977A mutants was confirmed to be labeled with radioactive CoASH and then with radioactive cysteine in the presence of 1−1382 or 1−1491 (data not shown) to validate monoaminoacylation capacity. The two point mutants of HMWP2

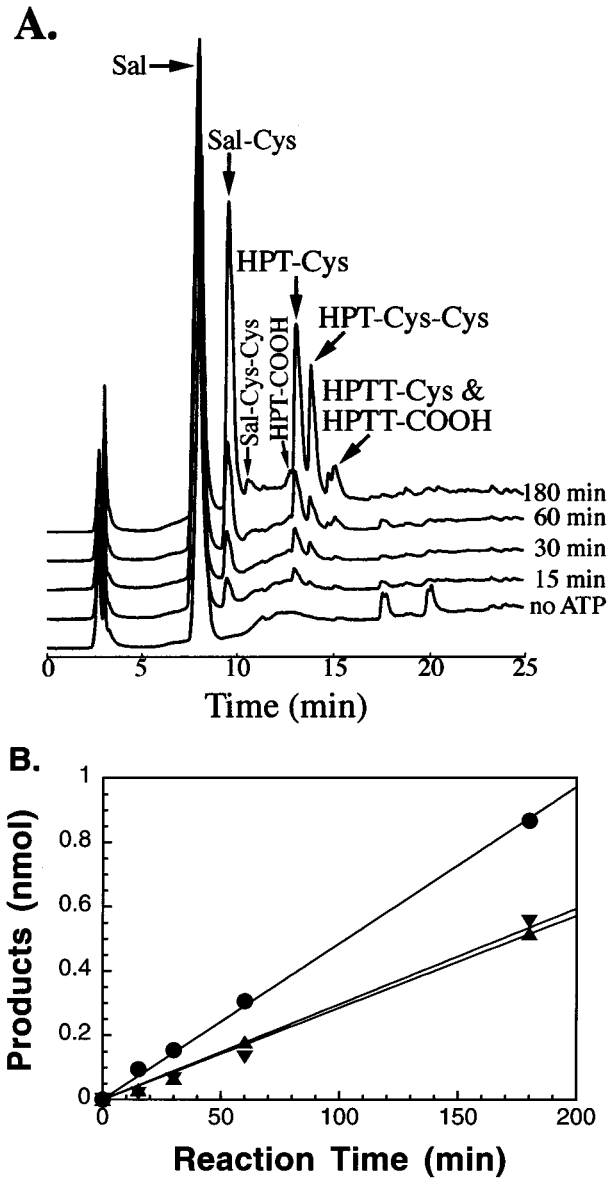

FIGURE 6: Time course of acyl-Cys intermediate formation catalyzed by wild-type 1−1382 (5 μM) and 1383−2035 (5 μM) at 30 °C in the presence of TCEP (2.5 mM), YbtE (0.5 μM), and the substrates L-cysteine (5 mM), salicylate (1 mM), and ATP (10 mM). (A) HPLC analysis of four time points and one control in the absence of ATP. The peaks at 9.5, 10.5, 12.8, 13.1, 13.8, and 15.1 min were identified by mass spectral analysis as Sal-Cys, Sal-Cys-Cys, HPT-COOH, HPT-Cys, HPT-Cys-Cys, and HPTT-Cys/HPTT-COOH, respectively. The peaks of Sal-Cys, HPT-COOH, HPT-Cys, and HPTT-COOH were also verified by co-injection with synthetic standards. (B) Plot showing the linearity of the amount of HPT-Cys (●), HPT-Cys-Cys (▼), and HPTT-Cys/HPTT-COOH (▲) vs reaction time. From the solid lines, k_{obs} values of 0.057, 0.035, and 0.033 min^{-1} are calculated for the formation of HPT-Cys, HPT-Cys-Cys, and HPTT-Cys/HPTT-COOH, respectively, using a calculated concentration (0.858 μM) of the enzyme complex 1−1382/1383−2035 based on the K_M of 1−1382/S1977A (see Figure 8).

1383−2035 indeed exhibited different functions on mixing with holo 1−1382, YbtE, ATP, cysteine, and salicylate. As shown in Figure 7 when the PCP1 domain was in the apo form (S1439A), only Sal-Cys was released (trace c), consistent with the inability of the Sal-S-ArCP donor domain to skip PCP1 and transfer to cysteinyl-PCP2. The only fate for Sal-S-ArCP is the default thiolysis by cysteine, which

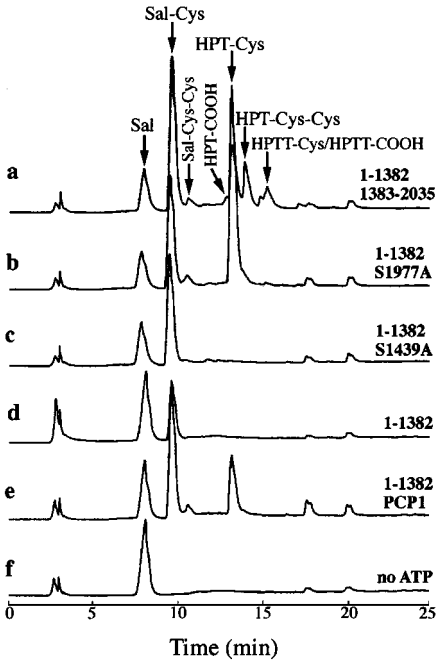

FIGURE 7: HPLC analysis of reaction products by different protein combinations in the presence of TCEP (2.5 mM), YbtE (0.5 μM), and the substrates L-cysteine (5 mM), salicylate (1 mM), and ATP (10 mM) at 30 °C for 10 h: (a) wild-type 1−1382 (5 μM)/1383−2035 (5 μM), (b) 1−1382 (5 μM)/S1977A (5 μM), (c) 1−1382 (5 μM)/S1439A (5 μM), (d) 1−1382 (5 μM), (e) 1−1382 (5 μM)/PCP1 (10 μM), and (f) wild-type 1−1382 (5 μM)/1383−2035 (5 μM), without ATP. The peaks were identified as described in the legend of Figure 5.

was observed with 1−1382 alone (trace d). When PCP2 was inactivated (S1977A), release of Sal-Cys and HPT-Cys as well as a minor amount of Sal-Cys-Cys was detected (trace b). These products were also observed in the incubation of holo forms of 1−1382 and the single PCP1 domain (trace e). The detection of HPT-Cys and Sal-Cys-Cys confirms that Sal-S-ArCP was transferred to Cys-S-PCP1. The anticipated progressive upstream to downstream directionality of chain transfer from ArCP to PCP1 to PCP2 is thus validated in these in trans reconstitutions.

Catalytic Efficiency of 1−1382 with 1383−2035 or PCP1 as the Substrate. As shown in Figure 7, more HPT-Cys was formed in reconstitution of 1−1382 (5 μM) with S1977A (5 μM) (trace b) than with PCP1 (10 μM). This suggests that catalytic throughput of 1−1382 with 1383−2035 is higher than with the single 108-amino acid PCP1 domain. To verify this conclusion, the affinity of 1−1382 and 1383−2035 was estimated by determining the K_M of S1977A as a substrate for 1−1382. The 1−1382/S1977A pair produces HPT-Cys predominantly, rather than the mix of three products, due to kinetic partitioning in the wild-type 1−1382/1383−2035 reconstitution. When the concentration of the S1977A mutant of 1383−2035 was varied and the concentration of 1−1382 was held constant at 3 μM, a K_M of 20 μM was measured with a k_{cat} of 0.17 min^{-1} (panels A and B of Figure 8 and Table 4). The k_{cat} is comparable to the total flux rate of 0.125 min^{-1} measured for wild-type 1−1382/1383−2035 when the rates of all three products **3**−**5** are summed (see above). K_M for wild-type 1−1382/1383−2035 was also determined (less accurately) to be 9 μM, measured from saturation kinetics of formation of **3**−**5** (data not shown).

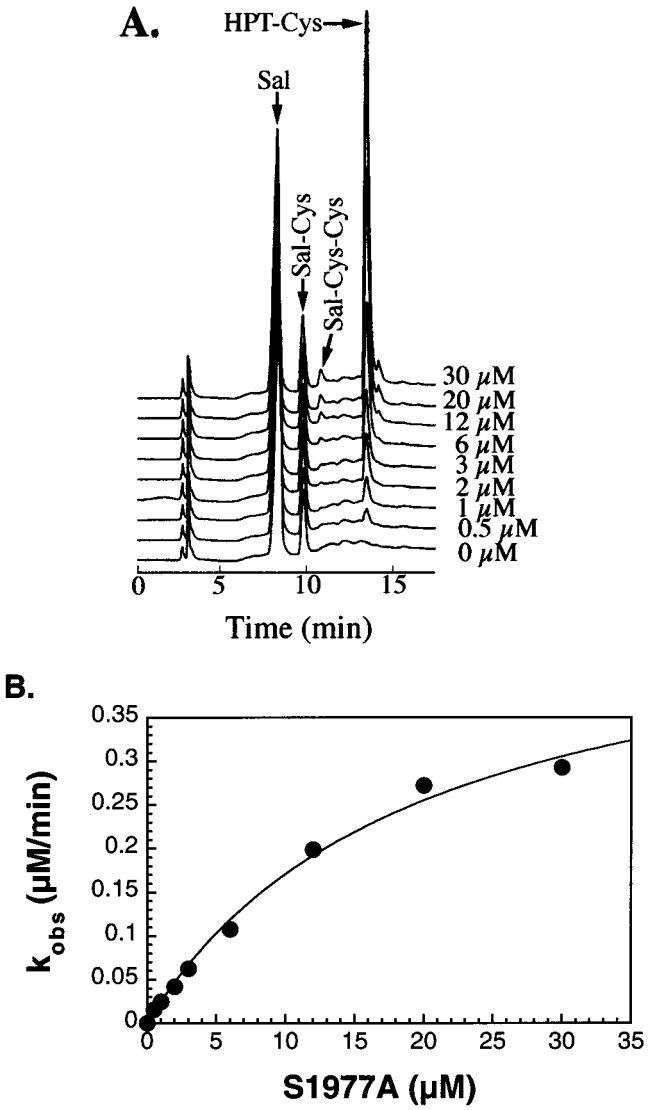

FIGURE 8: K_M measurement of 1−1382/S1977A in the presence of TCEP (2.5 mM), YbtE (0.5 μM), and the substrates L-cysteine (5 mM), salicylate (1 mM), and ATP (10 mM) at 30 °C for 140 min. The concentration of S1977A was varied from 0 to 30 μM, while the concentration of 1−1382 was held constant at 3 μM. (A) HPLC analysis of reaction products. (B) Plot of k_{obs} vs S1977A concentration. From this curve, a k_{cat} of 0.17 min^{-1} and a K_M of 20 μM are calculated.

Table 4: Kinetic Parameters for Two Fragment Interactions in Trans at 30 °C[a]

enzyme	k_{cat} (min^{-1})	K_M (μM)	k_{cat}/K_M (μM^{-1} min^{-1})
1−1382/S1977A	0.17 ± 0.01	20 ± 3	0.0085
1−1382/PCP1	0.043 ± 0.005	44 ± 10	0.00098

[a] The concentration of 1−1382 was held constant at 3 μM, and K_M values are for S1977A and PCP1 substrates.

Holo forms of 1−1382 and PCP1 likewise produce a time- and concentration-dependent formation of HPT-Cys, **3** (data not shown). The K_M for the holo form of PCP1 in formation of **3** by 1−1382 was determined to be 44 μM (data not shown), and k_{cat} was 0.043 min^{-1} (Table 4). The catalytic efficiency of PCP1 is more than 8-fold smaller than that of 1383−2035 (Table 4), suggesting some favorable protein−protein interaction between 1−1382 and Cy2-PCP2 domains of 1383−2035.

The Thiolytic Release of Acyl-S-HMWP2 Intermediates by Cysteine Can Be Accelerated by DTT. To address whether the low rates of release of acyl-S-enzyme intermediates by cysteine to yield products **2**−**5** was due to rate-limiting capture by cysteine acting as a thiol from solution, an experiment was conducted with the same substrates (ATP, salicylate, and cysteine), but now with varying amounts of DTT added. First, the HMWP2 fragment 1−1491, primed with Ppant at both ArCP and PCP1 domains, was used since we have noted (*19*) that it can make and release HPT-Cys (by in cis acyl transfer of Sal-S-ArCP to Cys-S-PCP1) in competition with DTT while the in trans reaction was interdicted. As shown in panels A and B of Figure 9, DTT accelerates the formation of HPT-Cys 20-fold, from a basal rate of 0.08 min^{-1} up to a saturating value of 1.6 min^{-1} (Table 5), consonant with values we have seen earlier (*19*). Thus, the low k_{cat} values for rerouting of the cascade of acyl-S-HMWP2 intermediates by cysteine from solution may be limited by the thiolytic-releasing steps. The apparent saturation value of 33 mM for DTT in Figure 9B could be a weak binding site in the enzyme or merely the kinetic manifestation of the fact that some step other than thiolytic release of HPT-S-PCP1 (e.g., the chain translocation step from ArCP to PCP1) has now become rate-limiting. Analogously, when the 1−1382 holo fragment was assayed in the presence of DTT, the rate of Sal-Cys release increased from 0.04 min^{-1} to a saturating value of 0.49 min^{-1} (Table 5), again with an apparent K_M of 45 mM.

DISCUSSION

In this study, the 230 kDa multidomain nonribosomal peptide synthetase, HMWP2, participating in the biosynthetic assembly of the virulence-conferring siderophore of *Y. pestis*, has been dissected into two fragments, and Ybt assembly and chain translocation have been analyzed to detect intermediates and assign them to the three carrier protein waystations of HMWP2. The dissection point, between residues 1382 and 1383, was chosen on the basis of domain homology searches that indicated this as a likely border between the adenylation domain responsible for cysteine activation and the first PCP (PCP1) domain. It was anticipated and then experimentally validated that the 1−1382 fragment (ArCP-Cy1-A) would retain the ability to generate cysteinyl-AMP, although the catalytic efficiency is lower compared to that of the 1−1491 fragment, suggesting some lability for the native conformation. Transfer of the cysteinyl moiety to the Ppant-SH tethers in the PCP1 and PCP2 domains is in trans, and thus dependent on the 1383−2035 (PCP1−Cy2−PCP2) fragment, in its doubly primed, bis-phosphopantetheinylated form. This 653-residue, 75 kDa C-terminal fragment of HMWP2, in wild-type and mutant forms, has permitted evaluation of the roles of each of the two PCP domains and the two Cy domains in chain assembly and provides initial insights into the order and timing of chain translocation and heterocyclization. The function of Cy1 could be assessed by in trans chain translocation to and release from PCP1 in both the S1977A mutant of 1383−2035 and the PCP1 domain on its own, while Cy2 function was assayed in the wild-type 1383−2035 fragment. These experiments have allowed reconstitution of both monoheterocyclization and tandem bisheterocyclization activity of HMWP2.

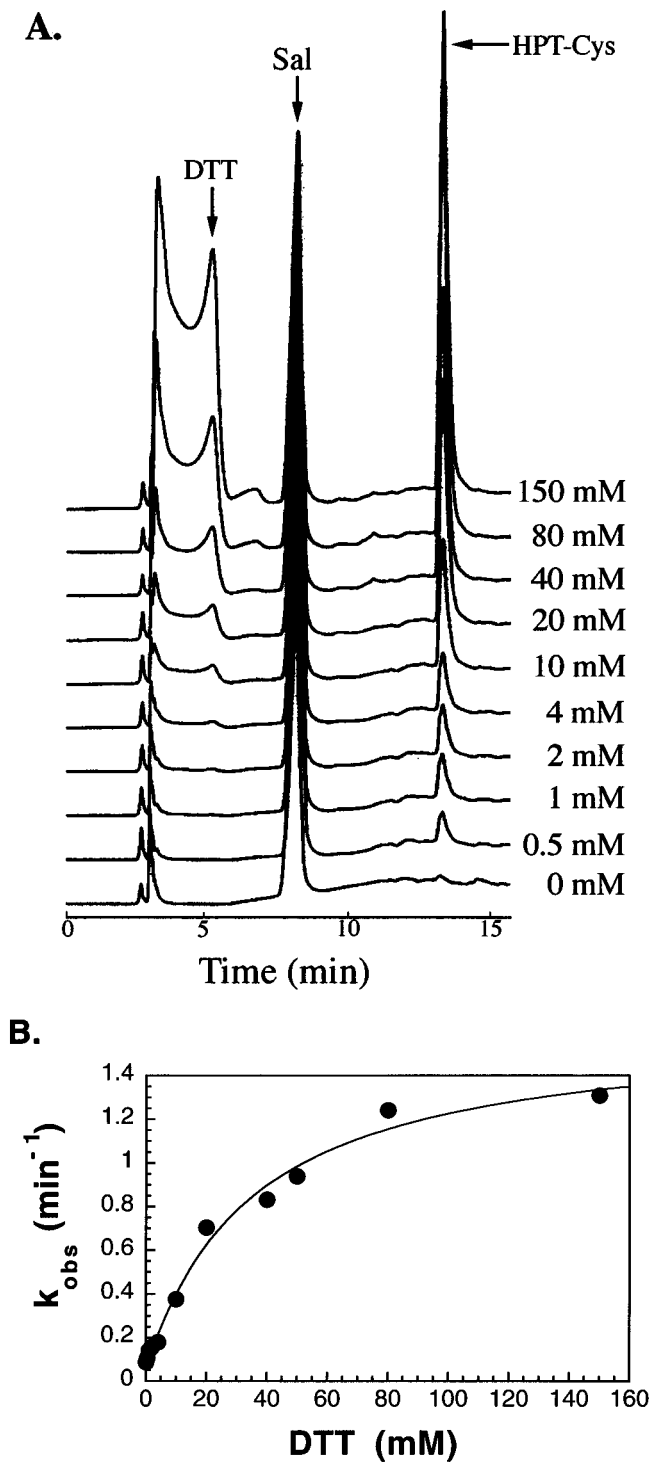

FIGURE 9: DTT acceleration of HPT-Cys formation by 1−1491 (0.5 μM) in the presence of DTT (0−150 mM), TCEP (2.5 mM), YbtE (0.25 μM), and the substrates L-cysteine (5 mM), salicylate (1 mM), and ATP (10 mM) at 30 °C for 60 min. (A) HPLC trace series. (B) Velocity of HPT-Cys formation vs DTT concentration. From this curve, a k_{cat} of 1.6 min^{-1} for HPT-Cys formation and an apparent K_M of 33 mM for DTT binding are calculated.

The key to assessment of both carrier and catalytic domain functions has been the ability of cysteine not only to act as a substrate for adenylation domain activation and transfer to the holo forms of each PCP domain but also to effect the slow thiolytic discharge of the cascade of elongating acyl-S-enzyme intermediates on all three of the carrier protein thiol waystations of HMWP2 fragments. The turnover rates

Table 5: Kinetic Parameters of Acyl-S-Enzyme Cleavage by DTT at 30 °C[a]

enzyme	k_{cat} (min^{-1})	K_M (mM)	k_{cat}/K_M (mM^{-1} min^{-1})
1−1382	0.49 ± 0.04	45 ± 16	0.011
1−1491	1.6 ± 0.1	33 ± 10	0.048

[a] Enzyme concentrations were 0.5 μM for 1−1491 and 1.0 μM for 1−1382, and K_M values are for the substrate DTT.

are slow, limited by the adventitious capture of acyl-S-enzyme intermediates by cysteine attacking from solution (after all, the purpose of these multimodular synthetases is to prevent unwanted discharge of these activated acyl-S-enzyme species to nonspecific nucleophiles), but the rerouting is mechanistically diagnostic. Multiple turnovers do take place during the incubations, establishing that this is catalytic throughput. The thiolytic interception by cysteine is then followed by intramolecular S to N migration of the acyl chains to fix them in hydrolytically stable linkages on the cysteine amino group, allowing detection and separation by HPLC and mass spectrometric characterization to validate structure. In our previous work on the 1−1491 fragment (*19*), we noted that lowering the cysteine concentration permitted hydrolysis to compete with thiolysis for discharge of the HPT-S-PCP1 species. The hydrolysis products detected here are minor components of the released set, in line with slow rates of chain release by the stronger thiol nucleophile. Replacement of the thiol-containing reducing agent DTT with the phosphine TCEP allowed detection of products **3**−**6** presumably by removing DTT as a thiolysis competitor for cysteine. Conversely, at high DTT levels, the extent of acyl-S-enzyme intermediate breakdown can be increased up to 20-fold so there is a balance between formation and decay of the cascade of acyl-S-enzyme intermediates. The catalytic efficiency of the two fragments, 1−1382 and 1383−2035, on reconstitution in trans is therefore modest, and the K_M value for the 75 kDa PCP−Cy2−PCP2 fragment is high (10−20 μM), limiting the preparative utility until improvements in protein−protein recognition are achieved.

Evidence for up to five acyl-S-enzyme intermediates is obtained by release and capture by cysteine during turnover from various fragments or combinations of fragments: Sal-Cys (**2**), Sal-Cys-Cys (**6**), HPT-Cys (**3**), HPT-Cys-Cys (**4**), and HPTT-Cys (**5**). These observations suggest the sequence in Scheme 4 for the timing and location of the assembling Ybt acyl chains on HMWP2. The most N-terminal domain (residues 1−100) is the ArCP, phosphopantetheinylated at the consensus serine site, Ser52. In holo 1−1382, this ArCP is the only thiol waystation. YbtE, the partner protein and salicylate ligase in the Ybt system, generates Sal-AMP and transfers it selectively to produce Sal-S-ArCP (*19*), as the first acyl-S-enzyme species, at the most upstream site. Thus, when cysteine is added to Sal-S-1-1382, it can produce a transthiolation−acyl thioester interchange and release Sal-Cys (**2**) as a diagnostic marker for the Sal-S-enzyme. The Sal-AMP in the active site of YbtE is not readily accessible to adventitious capture by the thiolate of cysteine, as evidenced by the k_{cat} of 0.0021 min^{-1} versus the rate of 94 min^{-1} (*19*) for thiolytic capture by the Ppant thiol of its specific partner domain, the N-terminal ArCP region of HMWP2, a 5 order of magnitude specificity.

When the salicyl moiety of Sal-S-ArCP is subsequently transferred to the next thiol waystation, PCP1, it is purport-

Scheme 4

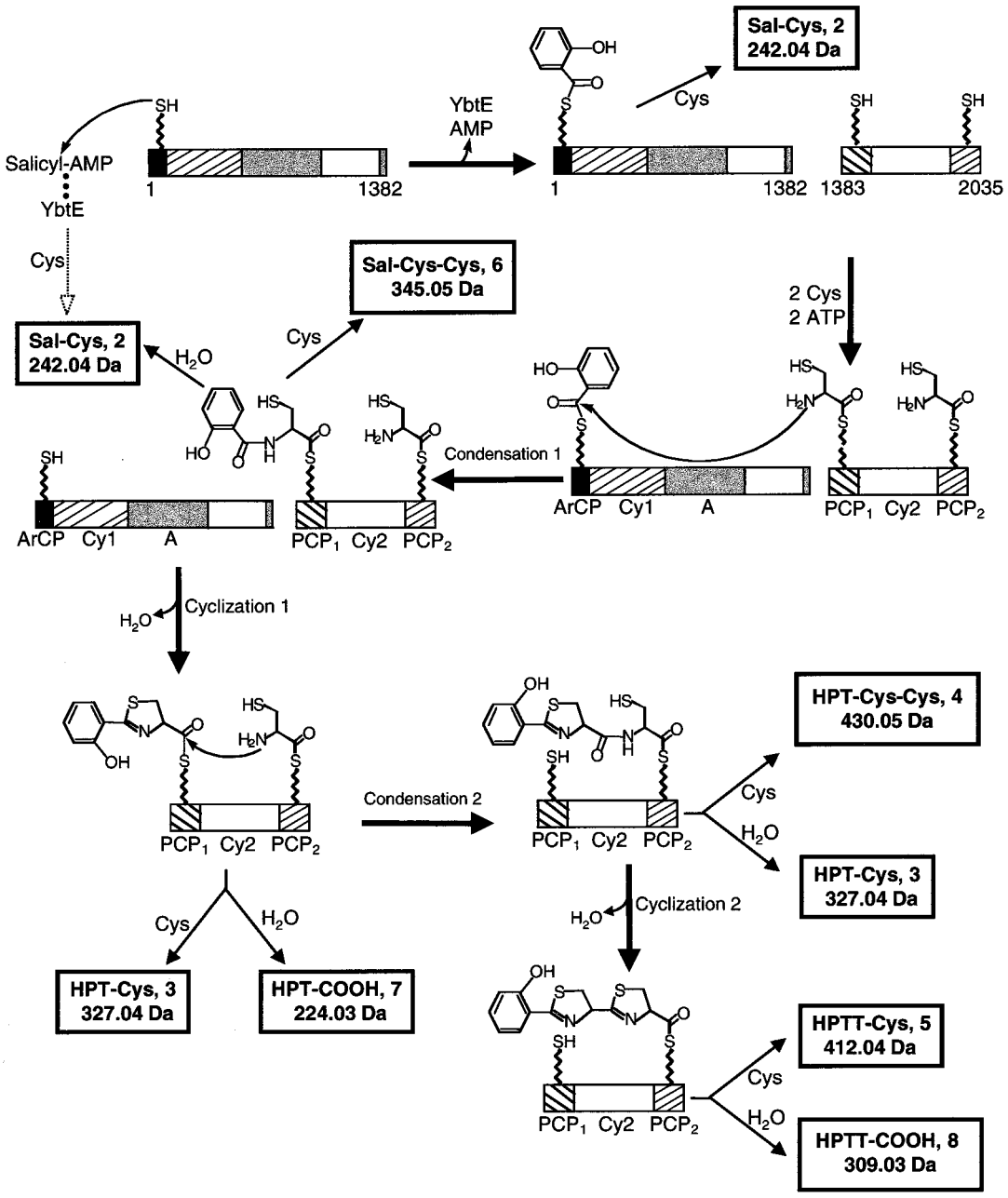

edly captured by the nucleophilic (deprotonated) amino group of Cys-S-PCP1, to produce the Sal-Cys-S-PCP1 as a transient precursor to the cyclized and dehydrated HPT-S-enzyme docked still at the PCP1 Ppant arm. Both amide bond formation (Sal-Cys) and cyclodehydration (Sal-Cys to HPT) can be attributed to catalysis by Cy1. A small amount of Sal-Cys-Cys (**6**) is detected and thought to reflect thiolytic capture of the sal-cys-S-PCP1 before its cyclization to the HPT-S-PCP1 acyl-S-enzyme which can be captured and released in thioester interchange by cysteine followed by S to N shift, to yield HPT-Cys (**3**). We have previously detected catalytic release of HPT-Cys by the 1−1491 fragment of HMWP2 where Cy1 and PCP1 are in cis so the in trans transfer was anticipated. In the absence of DTT, the in cis and in trans release rates of **3** are comparable (0.087 vs 0.057 min^{-1}) and likely limited not by the chemical steps in chain assembly but by the bimolecular thiolysis capture. The K_M value for holo-PCP1 acting as a salicyl chain acceptor during formation of **3** was 20 μM in the context of the 653-residue fragment and 44 μM when the 109-residue PCP1 was supplied as a small fragment.

The two products that were subsequently released, HPT-Cys-Cys (**4**) and HPTT-Cys (**5**), were novel and particularly informative. In particular, HPTT-Cys has the tandem 4,2-bisheterocyclic system characteristic of Ybt and must have arisen formally from tandem cyclodehydration of a Cys-Cys precursor (in this case, via an HPT-Cys-S-enzyme as an immediate precursor). HPTT-Cys is not detected in the combination of 1−1382 and the S1977A mutant of 1383−2035 fragment, consistent with the interpretation that the acyl chain must reach PCP2 before undergoing the formation of the second heterocycle. The studies with the S1439A and S1977A point mutants in PCP1 and PCP2, respectively, have validated that both PCP1 and PCP2 in the 75 kDa fragment are functional sites of cysteinylation. Thus, the mechanistic scheme of Scheme 4 assigns Cy2 the role of conversion of

HPT-Cys-S-PCP2 to HPTT-S-PCP2 by cyclodehydration, which is analogous to that practiced by Cy1 when the chain was docked upstream at PCP1. The thioester interchange of HPTT-S-PCP2 with cysteine in solution produces the diagnostic product HPTT-Cys (**5**) which can be detected by HPLC and LC−MS. It would appear that the cyclodehydrative conversion of HPT-Cys-S-PCP2 to HPTT-S-PCP2 is slow enough in the in trans reconstitution incubations that a fraction of the HPT-Cys-S-PCP2 can be captured and diverted by cysteine to yield HPT-Cys-Cys (**4**), analogous to the partition of the uncyclized and cyclized acyl-enzyme species at the upstream PCP1 carrier site. The HPT-Cys-Cys and HPTT-Cys formations are most intriguing, because they give the first evidence that Cy2 is functional in the 1383−2035 fragment and are consistent with condensation preceding cyclization. In the absence of YbtE, there is no indication of the HPTT-COOH or HPTT-Cys product (by MS analysis, data not shown), suggesting that Cy2 cannot condense a free cysteine but needs an aryl-N-cap, e.g., HPT-S-PCP1, as the upstream donor for Cys-S-PCP2 to act as the downstream acceptor and gives some constraint on determinants for how these assembly line catalysts control when a chain elongation step is carried out. This is a general problem to be solved for NRPS and PKS so that they do not start chains in the middle. Likewise, the Sal-S-ArCP acyl group does not serve as a donor to the Cys-S-PCP2 site in this two-fragment reconstitution system. Perhaps the Cy2 domain cannot catalyze the amide-forming acyl transfer because the acyl-S-ArCP and acyl-S-PCP2 chains cannot approach each other in the three-dimensional architecture of this assembly line catalyst. In this in trans two-fragment reconstitution of HMWP2, the ratio of the rate of HPT-Cys release to that of HPT-Cys-Cys and HPTT-Cys/HPTT-COOH of 0.057 to 0.035 + 0.033 min^{-1} (Table 2) suggests an about 50/50 split of occupancy of PCP1 and PCP2 carrier sites by elongating acyl chains, if thiolysis rates are assumed to be equivalent.

Assembling all the information from the two fragments of HMWP2 in wild-type and mutant forms validates the expectation (*11*, *28*) of a cascade of elongating acyl-S-enzymes, translocating from the N- to C-terminus of the multimodular NRPS subunit. The thiol waystations ArCP, PCP1, and PCP2 have differentiated functions. ArCP is the chain-initiating carrier protein site and the source of the aryl-N-cap on the growing natural product acyl chain. PCP1, after cysteinylation, is first the acceptor in the first amide bond formation (to make Sal-Cys), and then the substrate for cyclodehydration, and third the donor of the HPT-Cys acyl chain in the next translocation. PCP2 is, analogously, the downstream acceptor (as Cys-S-PCP2) for chain transfer and the locus for amide bond formation (HPT-Cys-S-PCP2), and then cyclodehydration (to HPTT-S-PCP2). While this completes the migration and growth of the three-ring HPTT moiety of Ybt on the most downstream of the six domains of the HMWP2 subunit, it is presumably also the jumping off point for intersubunit transfer of the acyl chain to the nine-domain HMWP1 subunit (Figure 1) where a malonyl-S-ACP intermediate is likely to be the nucleophilic acceptor for C−C bond formation in the PKS phase of the assembly line (*11*) which produces yersiniabactin. The ability to generate the covalent HPTT-S-enzyme species in the 1383−2035 fragment of HMWP2 described here should be a useful launching point for study of the NRPS−PKS interface between HMWP2 and HMWP1 in yersiniabactin synthesis, with generality for other hybrid NRPS−PKS synthetases for understanding their molecular bases of recognition.

ACKNOWLEDGMENT

We thank Prof. Robert D. Perry and Edward DeMoll of the University of Kentucky (Lexington, KY) for samples of yersiniabactin and Amy M. Gehring for providing PCP1 protein and the clone of HMWP2 1−1491.

REFERENCES

1. Drechsel, H., Stephan, H., Lotz, R., Haag, H., Zähner, H., Hantke, K., and Jung, G. (1995) *Liebigs Ann. Chem. 1995*, 1727−1733.
2. Chambers, C. E., McIntyre, D. D., Mouck, M., and Sokol, P. A. (1996) *BioMetals 9*, 157−167.
3. Jackson, S., and Burrows, T. W. (1956) *Br. J. Exp. Pathol. 37*, 577−583.
4. Perry, R. D., and Fetherston, J. D. (1997) *Clin. Microbiol. Rev. 10*, 35−66.
5. Bearden, S. W., Fetherston, J. D., and Perry, R. D. (1997) *Infect. Immun. 65*, 1659−1668.
6. Fetherston, J. D., Lillard, J. W., Jr., and Perry, R. D. (1995) *J. Bacteriol. 177*, 1824−1833.
7. Haag, H., Hantke, K., Drechsel, H., Stojiljkovic, I., Jung, G., and Zähner, H. (1993) *J. Gen. Microbiol. 139*, 2159−2165.
8. Chambers, C. E., and Sokol, P. A. (1994) *J. Clin. Microbiol. 32*, 32−39.
9. Guilvout, I., Mercereau-Puijalon, O., Bonnefoy, S., Pugsley, A. P., and Carniel, E. (1993) *J. Bacteriol. 175*, 5488−5504.
10. Pelludat, C., Rakin, A., Jacobi, C. A., Schubert, S., and Heesemann, J. (1998) *J. Bacteriol. 180*, 538−546.
11. Gehring, A. M., DeMoll, E., Fetherston, J. D., Mori, I., Mayhew, G. F., Blattner, F. R., Walsh, C. T., and Perry, R. D. (1998) *Chem. Biol. 5*, 573−586.
12. Donadio, S., Staver, M. J., McAlpine, J. B., Swanson, S. J., and Katz, L. (1991) *Science 252*, 675−679.
13. Marahiel, M. A., Stachelhaus, T., and Mootz, H. D. (1997) *Chem. Rev. 97*, 2651−2673.
14. Walsh, C. T., Liu, J., Rusnak, F., and Sakaitani, M. (1990) *Chem. Rev. 90*, 1105−1129.
15. von Döhren, H., Keller, U., Vater, J., and Zocher, R. (1997) *Chem. Rev. 97*, 2675−2705.
16. Cox, C. D., Rinehart, K. L., Jr., Moore, M. L., and Cook, J. C., Jr. (1981) *Proc. Natl. Acad. Sci. U.S.A. 78*, 4256−4260.
17. Stubbe, J., and Kozarich, J. W. (1987) *Chem. Rev. 87*, 1107−1136.
18. Vanderwall, D. E., Lui, S. M., Wu, W., Turner, C. J., Kozarich, J. W., and Stubbe, J. (1997) *Chem. Biol. 4*, 373−387.
19. Gehring, A. M., Mori, I., Perry, R. D., and Walsh, C. T. (1998) *Biochemistry 37*, 11637−11650.
20. Konz, D., Klens, A., Schörgendorfer, K., and Marahiel, M. A. (1997) *Chem. Biol. 4*, 927−937.
21. Quadi, L. E. N., Weinreb, P. H., Lei, M., Nakano, M. M.., Zuber, P., and Walsh, C. T. (1998) *Biochemistry 37*, 1585−1595.
22. Lambalot, R. H., Gehring, A. M., Flugel, R. S., Zuber, P., LaCelle, M., Marahiel, M. A., Reid, R., Khosla, C., and Walsh, C. T. (1996) *Chem. Biol. 3*, 923−936.
23. Gehring, A. M. (1998) Ph.D. Dissertation, Harvard Medical School, Boston, MA.
24. Ho, S. N., Hunt, H. D., Horton, R. M., Pullen, J. K., and Pease, L. R. (1989) *Gene 77*, 51−59.
25. Gehring, A. M., Bradley, K. A., and Walsh, C. T. (1997) *Biochemistry 36*, 8495−8503.
26. Gehring, A. M., Mori, I., and Walsh, C. T. (1998) *Biochemistry 37*, 2648−2659.
27. Kirley, T. L. (1989) *Anal. Biochem. 180*, 231−235.
28. Cane, D. E., Walsh, C. T., and Khosla, C. (1998) *Science 282*, 63−68.

BI991574N